Available online at www.sciencedirect.com
ScienceDirect
Ceramics International 38 (2012) 561–570
CERAMICS INTERNATIONAL
www.elsevier.com/locate/ceramint

Comparison of DOPA and DPPA liposome templates for the synthesis of calcium phosphate nanoshells

Chiew-Hwee Yeo [a], Sharif Hussein Sharif Zein [a,*], Abdul Latif Ahmad [a], David S. McPhail [b]

[a] School of Chemical Engineering, Engineering Campus, Universiti Sains Malaysia, Seri Ampangan, 14300 Nibong Tebal, Seberang Perai Selatan, Pulau Pinang, Malaysia
[b] Department of Materials, Imperial College London, Prince Consort Road, London SW7 2AZ, UK

Received 1 April 2011; received in revised form 21 July 2011; accepted 22 July 2011
Available online 29th July 2011

Abstract

The aim of this paper is to synthesise calcium phosphate (CaP) nanoshells by controlling their particle size and shape using negatively charged liposomes (1,2 dioleoyl-*sn*-glycero-3 phosphate sodium salt (DOPA) and 1,2-dipalmitoyl-*sn*-glycero-3-phosphate sodium salt (DPPA)) as a template. The morphology, particle size, size distribution and zeta potential properties of DOPA and DPPA liposome templates were determined. The results showed that both DOPA and DPPA formed spherical nanoshell structures to be used as templates for the synthesis of CaP nanoshells. By using the DOPA template, spherical CaPs structures with a mean particle size of 197.5 ± 5.8 nm were successfully formed. In contrast, needle or irregularly shaped CaP particles were observed when using the DPPA template.

Keywords: Calcium phosphates; Nanoshells; Liposomes; Template

1. Introduction

Since 2000, more than five thousand research papers have been published related to the synthesis of calcium phosphates (CaPs), according to the Scopus database. Due to their compositional similarity with the mineral phase of bone, CaPs have a significant role in the field of bone tissue engineering [1]. In addition, they have excellent biological properties such as non-toxicity, biocompatibility and osteoconductivity [1,2]. However, the fracture toughness values of synthetic CaP ceramics are not as high as those of human cortical bone. Therefore, CaP ceramics lack sufficient strength to be used at high-load bearing sites, such as femoral and tibial bones [3]. Researchers are now focusing on finding similar materials that fulfil the requirements of bone. Properties of existing CaPs can be improved by exploring the unique advantages of nanotechnology. It has been established that nanotechnology offers a distinct approach to overcome the deficiencies of CaPs [1].

Nanostructured materials have proven to be biologically effective [4]. Nanostructured ceramics clearly represent a promising class of orthopedic and dental implant formulations with enhanced biological and biomechanical performance [1]. Indeed, greater mechanical properties have been reported by reducing the grain size of ceramics to the nanometer range [5,6]. Subsequently, improved properties are also possible by controlling their characteristics such as particle size, particle distribution and agglomeration [7]. For example, nanostructured hydroxyapatite (HA) can promote osteoblast adhesion and proliferation, osseointegration, and the deposition of calcium containing minerals on the surface of these materials [8].

Various nanostructures of CaP ceramics with Ca/P molar ratios of 0.50–2.00 [9], including spherical nanoparticles [10], nanowires [11], nanorods [12,13], and nanoneedles [14], have been synthesised in the laboratory with different synthesis methods. However, only a few attempts have been made to prepare nanoshell structures of CaPs. Nanoshells can be defined as a rigid shell surrounding a solid and/or liquid spherical core composed of a different material. They range in size from 20 nm to 200 nm [15]. In addition, they have been found to be very useful in various fields such as ion exchangers, catalysts, drug delivery and especially bone scaffolds [16–18].

* Corresponding author. Tel.: +60 4 599 6442; fax: +60 4 594 1013.
E-mail address: chhussein@eng.usm.my (S.H.S. Zein).

0272-8842/$36.00
doi:10.1016/j.ceramint.2011.07.044

Because the biological and mechanical properties of CaP particles are expected to be strongly influenced by their particle size and shape [19], the shape and size control are important in the synthesis method. Thus, the aim of this study was to synthesise CaP nanoshells and control their particle size and shape by using negatively charged liposomes (1,2 dioleoyl-*sn*-glycero-3 phosphate sodium salt (DOPA) and 1,2-dipalmitoyl-*sn*-glycero-3-phosphate sodium salt (DPPA)) as templates through the base titration method. These liposomes were chosen to make a template due to their negatively charged head group, which can help in the localisation of calcium and phosphate ions around the liposomes and allow the growth of CaPs [20]. In addition, they have a good biocompatibility and have the ability to support the reparation of osseous deficiencies [21]. Furthermore, they have strong intrinsic bioactivity, which can be used in bone reconstruction or antibiotic filled porous coatings for implants and may find benefit in creating artificial bones [22].

2. Materials and methods

2.1. Materials

Calcium chloride ($CaCl_2$), 85% phosphoric acid (H_3PO_4) and sodium hydroxide (NaOH) were commercially obtained from Sigma–Aldrich. DOPA ($C_{39}H_{72}O_8PNa$) lipid was supplied from Avanti Polar Lipids and DPPA ($C_{35}H_{68}O_8PNa$) lipid was obtained from Fluka. Glycerol (3% (v/v)) was supplied from Merck. All chemicals were of a commercial analytical grade. De-ionised (DI) water was used as a solvent in the experiments.

2.2. Methods

The synthesis of CaP nanoshells was performed in two steps. First, the liposome template was prepared by using the DOPA or DPPA lipid. Then, the prepared template was used to synthesise the CaP nanoshells.

2.2.1. Preparation of liposome templates

The preparation of the DOPA liposome template was performed using the sonication method developed by Schmidt [23]. Sonication was used to reorganise the multilamellar (multiple bilayer) to unilamellar (single bilayer) liposome templates to reduce their size and improve their size distribution. The procedures were performed at room temperature because the DOPA lipid has low T_c (−8 °C). First, DOPA lipids were hydrated in a scintillation vial of DI water. Second, the hydrated DOPA solutions were stirred at 1000 rpm for 1 h. Finally, the hydrated DOPA solutions were sonicated in an ultrasonic bath for 15 min.

The DPPA liposome template was prepared by using the same preparation method as that of the DOPA template. However, the DPPA lipid could not dissolve in the solutions homogenously due to its high T_c (67 °C). The formation of liposomes requires heating the liposomes at temperatures not lower than the T_c of the lipid [24]. Thus, considering the high T_c of the DPPA lipid, a combination of methods of sonication and heating was used. The heating method used was developed by Mozafari et al. [25]. First, the DPPA lipids were hydrated in a scintillation vial of DI water. Then, the hydrated DPPA solutions were stirred at 1000 rpm and heated at 120 °C for 1 h in the presence of glycerol (3% (v/v)). This procedure was conducted to ensure that all lipids were dissolved homogenously. Glycerol has the ability to increase the stability of lipid vesicles, and it does not need to be removed from the final liposome product [24]. The hydrated DPPA solutions were then placed in an ultrasonic bath and sonicated for 15 min above the T_c of the DPPA lipid. Finally, the hydrated DPPA solutions became translucent, and the DPPA solutions transformed from gel to liquid [26,27].

2.2.2. Synthesis of CaP nanoshells

CaP nanoshells with liposome templates were prepared using a modified base titration method developed Schmidt et al. [20,22,28]. First, 0.1 M of $CaCl_2$ and 0.1 M of H_3PO_4 (adjusted to pH 7 with 0.1 M of NaOH) were added separately to the prepared liposome template of DOPA or DPPA. The mixtures were then stirred at 400 rpm at room temperature. The concentrations of calcium and phosphate ions were fixed at 0.1 M to reach an initial molar ratio of Ca/P equal to 1. Next, 0.1 M of NaOH as a base solution was added into the mixtures every 30 min to allow the precipitation of CaPs on the liposomes. Approximately twenty 200-μl NaOH additions were used in each experiment. NaOH was used as base solution in this study to supersaturate the mixtures by increasing the pH of the mixtures. The pH changes during the experiments were measured using a pH meter (Eutech Instrument – Ecoscan pH 5). The mixtures were then stirred overnight and then ultrafiltered to separate the unwanted particles by using Whatman's membrane nucleopore track-etched polycarbonate with a 50 nm pore size from Fisher Scientific. Finally, before analysis, the mixtures were dried in an oven at 60 °C for 48 h to obtain the final product.

2.2.3. Characterisation of the liposome templates and CaP nanoshells

The morphology analyses of the liposome templates and CaP nanoshells were examined by transmission electron microscopy (TEM) (Philips, model CM 12) operating at 120 keV. Samples of the templates were prepared using the technique of negative staining in which 2% uranyl acetate was dropped into samples on a carbon-coated copper grid before air-drying, while the samples of CaP nanoshells were prepared by placing one drop of the sample dispersed in absolute ethanol on a carbon-coated copper grid and air drying.

The particle size of the liposome templates and CaP nanoshells were measured by using the technique of dynamic light scattering (DLS). In addition, the width of the size distribution was obtained using the polydispersity index. In addition, the zeta potential of the templates and CaP nanoshells were obtained by using the technique of laser Doppler velocimetry (LDV). DLS and LDV were measured on a Zetasizer Nano ZS (Malvern, UK). Briefly, the samples of

templates were diluted in DI water while the samples of CaP nanoshells in powder form were dispersed in DI water before addition to the sample cell. Each experiment was repeated in triplicate, and each datum given is the average of 15 runs. All the measurements were performed at room temperature.

The elemental analyses of the CaP nanoshells were examined by energy-dispersive X-ray spectrometry (EDX) (Leo Supra 35 VP FESEM). A sample in powder form was spread evenly on the top of a double-sided carbon tape in which the tape was attached to an aluminium stub. The weight percentages of elements of samples were obtained as an average of 3 values in the EDX results.

Infrared spectra of the samples of CaP nanoshells were obtained in the transmission mode using a Fourier transform infrared (FT-IR) Perkin-Elmer spectrometer model Spectrum GX from discs containing samples of CaP nanoshells and potassium bromide (KBr) in the range 4000 cm^{-1} to 400 cm^{-1}. For sample preparation, powder samples were first mixed with KBr and were pressed to form a thin pellet for analysis.

3. Results and discussion

3.1. Characterisation of liposome templates

To act as a template for CaP nanoshells, the liposomes should have stable spherical structures, which allow the CaPs to grow uniformly on them. The structures of the liposome templates were observed via TEM analysis in Fig. 1(a–c). Fig. 1(a) shows that the spherical unilamellar template structures successfully formed from the DOPA lipid, although there were some aggregates. However, as shown in Fig. 1(b), spherical unilamellar template structures were not obtained when the DPPA lipid was prepared similarly to the DOPA lipid; this finding might due to the gel state of the DPPA lipid, which could not form closed continuous bilayered structures when the preparation temperature was under the T_c of DPPA lipid [24]. However, when the DPPA lipids were mixed with glycerol and heated above its T_c, spherical unilamellar structures of DPPA liposome template were successfully formed (Fig. 1(c)). This may due to the interaction energy between the chains reduced and the fluidity of liposomes increased during the heating process (above T_c of DPPA lipids) [29,30]. As a result, the liposomes can be reorganised to form unilamellar structures by sonication.

The TEM images are of little use for evaluating absolute sizes because the liposomes may be distorted by the vacuum, and the high-energy electron beam used in imaging could, in principle, damage the liposome structures [31]. To address the issue, the samples were characterised using a Zetasizer Nano ZS to obtain information on their size and size distribution. In addition, evaluation of the zeta potential of the liposome templates using the Zetasizer Nano ZS can help to predict their stability [27].

The results of the mean of particle size, polydispersity index (width of the particle size distribution) and zeta potential measurements of the DOPA and DPPA templates are summarised in Table 1. The DOPA template had a smaller mean particle size (64.7 ± 0.7 nm) compared to the DPPA template (103.9 ± 1.5 nm). Thus, both DOPA and DPPA templates are categorised as unilamellar liposomes because

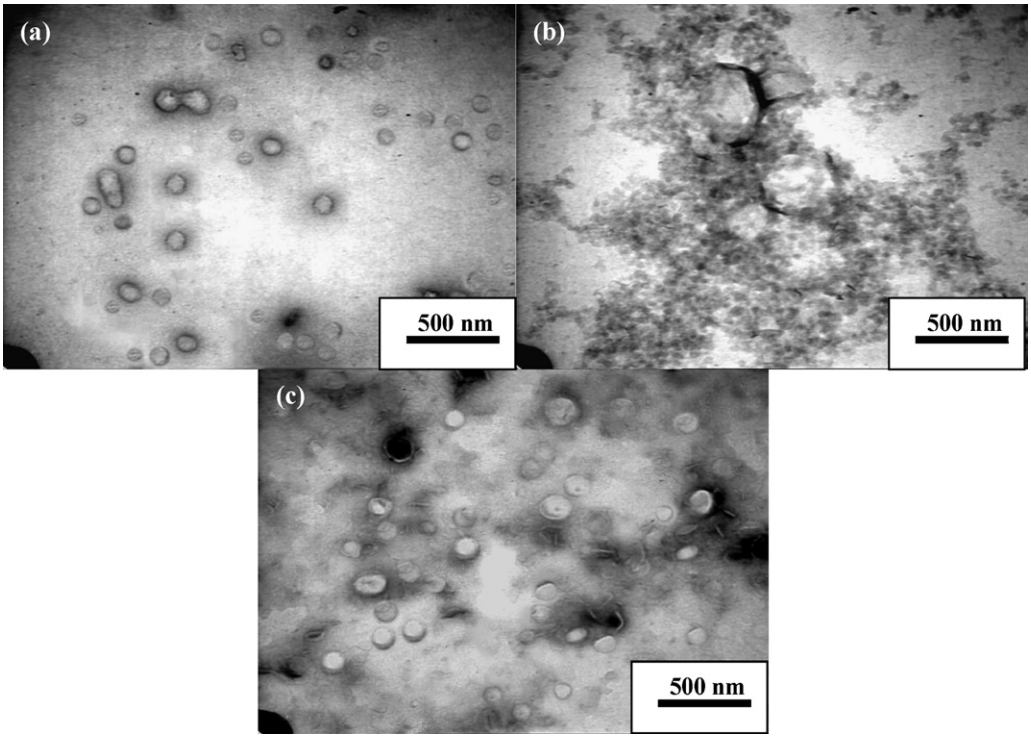

Fig. 1. TEM images of liposome templates (a) DOPA (without heating and glycerol), (b) DPPA (without heating and glycerol), and (c) DPPA (with heating and glycerol).

Table 1
The mean of particle size, polydispersity index and zeta potential of DOPA and DPPA liposome templates.

	DOPA	DPPA
Particle size (nm)	64.7 ± 0.7	103.9 ± 1.5
Polydispersity index	0.235 ± 0.013	0.275 ± 0.008
Zeta potential (mV)	−75.3 ± 2.9	−53.2 ± 3.0

Note: Each type of liposome was measured three times.

their particles sizes were less than 500 nm [32]. In addition, the mean polydispersity index values of DOPA and DPPA templates were similar, indicating that both liposomes had similar particle size distributions. In addition, the particles sizes of the templates of the DOPA (Fig. 2(a)) and DPPA (Fig. 2(b)) were in the ranges between 13.6–255.0 nm and 13.6–531.2 nm, respectively. On the other hand, the mean zeta potentials of the DOPA and DPPA templates were −75.3 ± 2.9 mV and −53.2 ± 3.0 mV, respectively (Table 1). Liposome templates with a zeta potential more negative than −30 mV are normally considered stable [33]. The stable and negatively charged templates of DOPA and DPPA can aid the localisation of ions around the liposomes and enhance the local supersaturation of CaPs [34]. Thus, it is assumed that the zeta potentials of the DOPA and DPPA templates are sufficiently negative to enhance the precipitation of CaPs nanoshells on them [35]. In conclusion, both DOPA and DPPA liposomes were determined to be suitable templates for nanoshell based materials.

3.2. Characterisation of CaP nanoshells

Fig. 3 shows the pH as a function of the number of NaOH additions (1 addition = 200 μl of 0.1 M of NaOH) for the synthesis of CaP nanoshells using DOPA and DPPA templates.

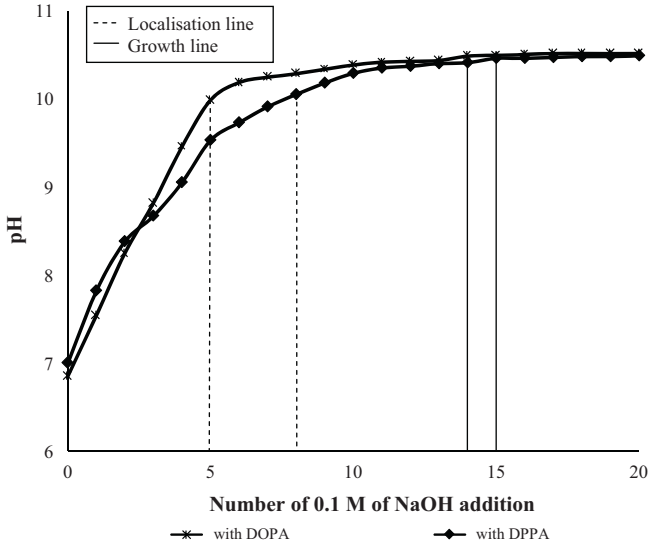

Fig. 3. pH as a function of the number of NaOH additions for DOPA and DPPA templates in the synthesis of CaP nanoshells (1 addition = 200 μl of 0.1 M of NaOH).

Generally, the pH of the mixtures varied in three stages (initiation, localisation and growth) in the synthesis of CaP nanoshells. At the initiation stage, the pH of the mixtures using DOPA and DPPA templates increased rapidly from 6.85 to 7.00, respectively. Then, the pH started to increase gradually from the 5th (pH 10.02) and 8th (pH 10.05) NaOH addition for the mixtures with DOPA and DPPA templates, respectively. Calcium and phosphate ions began to localise around the negative charges of liposomes at this localisation stage [20]. Finally, the mixture reached the growth stage, which is the most important stage in the synthesis of CaP nanoshells because the growth of CaPs on liposome templates can take place once the

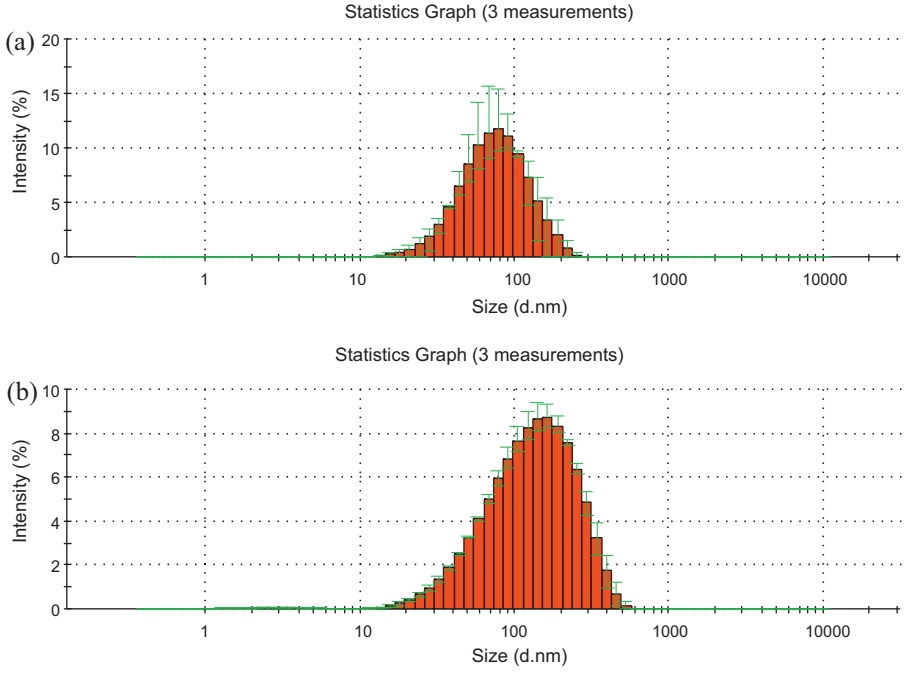

Fig. 2. Particle size distributions of liposome templates of (a) DOPA and (b) DPPA.

Table 2
Comparison of weight percentage of elements in samples of CaP nanoshells and their final molar ratios of Ca/P.

Sample of CaP nanoshells	Elements (wt.%)						Mole fraction of Ca	Mole fraction of P	Final molar ratio of Ca/P
	Ca	P	C	O	Na	Cl			
(a) With DOPA	12.64	10.36	26.76	36.90	12.23	1.11	0.32	0.33	0.97
(b) With DPPA	12.74	6.79	40.36	27.35	11.63	1.12	0.32	0.22	1.45

Note: The weight percentages of elementals of samples obtained as an average of three values according to EDX results.

pH is saturated and the supersaturation of the mixtures occurred [36]. The optimal pH was reached at the 14th (pH 10.52) and 15th (pH 10.49) NaOH addition for the mixtures with DOPA and DPPA templates, respectively, and was maintained until the 20th NaOH addition (end of the experiments). The optimal pH of both mixtures was very close to each other, although the mixture using DPPA had a higher initial pH than the mixture using DOPA as a template. Thus, the optimal pH of the mixtures did not depend on the types of liposome templates. However, the number of NaOH additions needed to reach localisation and growth stages for the mixture of CaP nanoshells using DOPA templates were less than that of DPPA template. Thus, it can be assumed that the time needed for the growth of CaPs on the DOPA template was less if compared with that of the DPPA template.

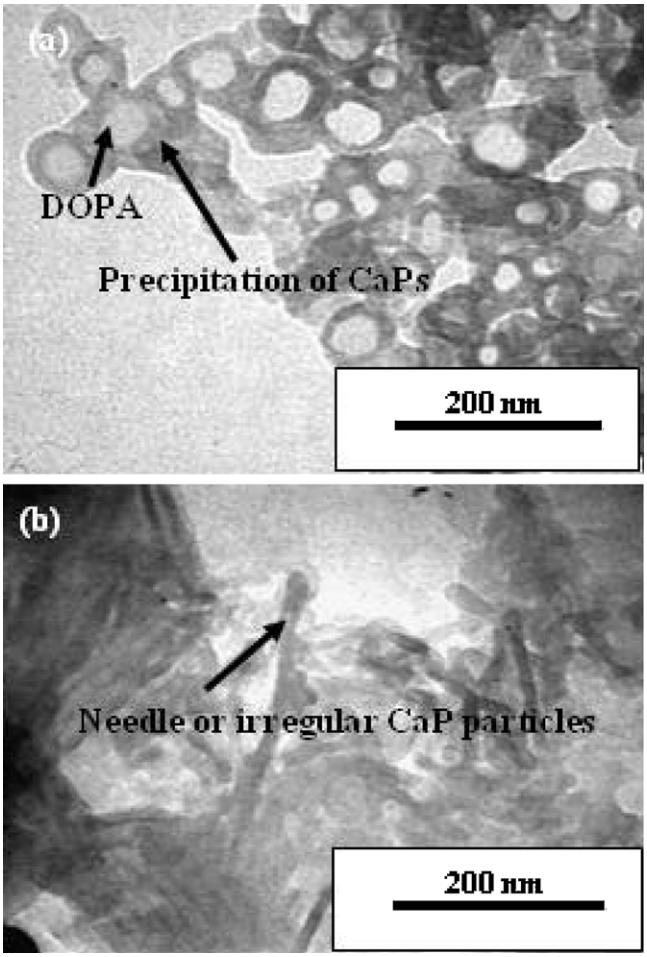

Fig. 4. TEM images of CaP nanoshells synthesised with templates of (a) DOPA and (b) DPPA.

Elemental analyses were performed using the EDX technique. The comparison of the weight percentage of elementals and their final molar ratio Ca/P of the CaP nanoshells using DOPA and DPPA templates are shown in Table 2. Calcium (Ca), phosphorus (P), carbon (C) and oxygen (O) are the main elements identified as the major constituents, as in bone, with some minor components of sodium (Na) and chloride (Cl). The high percentages of C in both samples are attributed to carbonate ions (CO_3^{2-}) in the samples and originate from the long chain of liposomes. The final molar ratio of Ca/P of the CaP nanoshells using the DOPA template (0.97) approaches the molar ratio of Ca/P of CaP nanoshells (1.00), which was suggested by Schmidt et al. [28]. This Ca/P molar ratio (1.00) could correspond to either crystalline brushite or amorphous calcium phosphate (ACP) [28,37,38]. On the other hand, CaP nanoshells using the DPPA template had a higher final molar ratio of Ca/P of (1.45), which corresponded to the calcium-deficient hydroxyapatite (CDHA) or ACP [1,39]. Thus, the difference in the molar ratio of Ca/P may influence the morphology of CaP nanoshells.

The TEM technique was employed to visualise the structural morphology of CaP nanoshells, and the images are shown in Fig. 4(a) and (b). In Fig. 4(a), TEM examination of CaP nanoshells using the DOPA template revealed that the CaPs precipitated at the outer layer of the vesicles. Dark field images confirmed the precipitation of CaPs. CaP nanoshells in spherical structures were formed using the DOPA template, although some aggregates were observed. On the other hand, needle or irregularly shaped nanoparticles of CaPs were observed in Fig. 4(b) when using the DPPA template. The needle or irregularly shaped particles were obtained due to the instability of the DPPA template because the spherical structure of the DPPA template may be damaged during the experiments. As a conclusion, DOPA had a better template effect on the growth of CaPs nanoshells than DPPA.

Table 3 shows the mean of particle size, polydispersity index and zeta potential values obtained for the samples CaP nanoshells using DOPA and DPPA templates. The results showed that the mean particle size of CaP nanoshells using the DOPA template (197.5 ± 5.8 nm) was significantly smaller than that using the DPPA template (1889.0 ± 301.7 nm). In addition, the mean particle sizes of the CaP nanoshells were increased from 64.7 ± 0.7 nm to 197.5 ± 5.8 nm and from 103.9 ± 1.5 nm to 1889.0 ± 301.7 nm after the growth of CaPs on the DOPA and DPPA templates, respectively.

Table 3
The mean of particle size, polydispersity index and zeta potential of CaP nanoshells using DOPA and DPPA templates.

	CaP nanoshells	
	With DOPA	With DPPA
Particle size (nm)	197.5 ± 5.8	1889.0 ± 301.7
Polydispersity index	0.326 ± 0.034	1.000
Zeta potential (mV)	−34.5 ± 0.6	−20.9 ± 0.5

Note: Each type of CaP nanoshells was measured three times.

In addition, the polydispersity index values were increased from 0.235 ± 0.013 to 0.326 ± 0.034 and from 0.275 ± 0.008 to 1.000 when CaPs were grown on DOPA and DPPA templates, respectively. CaP nanoshells using DPPA template are very polydisperse and may not be suitable for DLS measurements because this particle sizing technique has a limitation in describing the size of non-spherical particles. The non-spherical particles scatter differently than spherical particles and affect the diffusion speed, and thus the particle size will change [40]. Thus, the particle size of the needle or irregular particles of CaPs using the DPPA template may be significantly different than the original particle size of the DPPA template.

Fig. 5(a) and (b) shows the typical size distribution obtained from the CaP nanoshells using DOPA and DPPA templates, respectively. Two population sizes of CaPs particles can be observed for both samples. The main population shown in Fig. 5(a) composed 92.4% of the particles of CaP nanoshells and was obtained in the size range between 37.8 nm and 825.0 nm when using DOPA as the template. Meanwhile, the remaining particles were much larger in size, between 955.4 nm and 2669.0 nm. For CaP nanoshells using the DPPA template, the population shown in Fig. 5(b), composed of 34.0% of the smaller particles, was between 68.1 nm and 396.1 nm in size. Thus, up to 76.3% of the particles were larger particles with sizes in the range from 458.7 nm to 1718.0 nm. Thus, the CaP nanoshells produced using the DOPA template were more monodisperse than those using the DPPA template.

On the other hand, it was confirmed that the potential surface of CaP nanoshells did change significantly after the growth of CaP on liposome templates. The average zeta potentials of CaP nanoshells with DOPA and DPPA templates were −34.5 ± 0.6 mV and −20.9 ± 0.5 mV, respectively. However, the magnitude of the zeta potential of CaP nanoshells decreased from −75.3 ± 2.9 mV and −53.2 ± 3.0 mV after the growth of CaP on DOPA and DPPA templates, respectively. The results agree with the theory that the electrostatic potential is dependent upon the distance from the surface [41]. The slightly extended positive charge of calcium ions from the surface of liposomes increased the distance from the surface, resulting in the lower negative zeta potential of the CaP nanoshells. Moreover, the liposomes containing phosphatidic acid possess a specifically strong affinity for calcium ions. Thus, the zeta potential of the liposome template changed from strongly negative to weakly negative after binding calcium ions [42]. However, the result of the zeta potential of CaP nanoshells using the DPPA template (less negative than −30 mV) showed that the CaP nanoshells using the DPPA template may become unstable after the growth of CaPs on the DPPA template, perhaps because the growth of CaPs on the template was not uniform in every direction. Therefore, it can be assumed that spherical structures of particles were more stable than needle or irregular particles in the synthesis of CaP nanoshells.

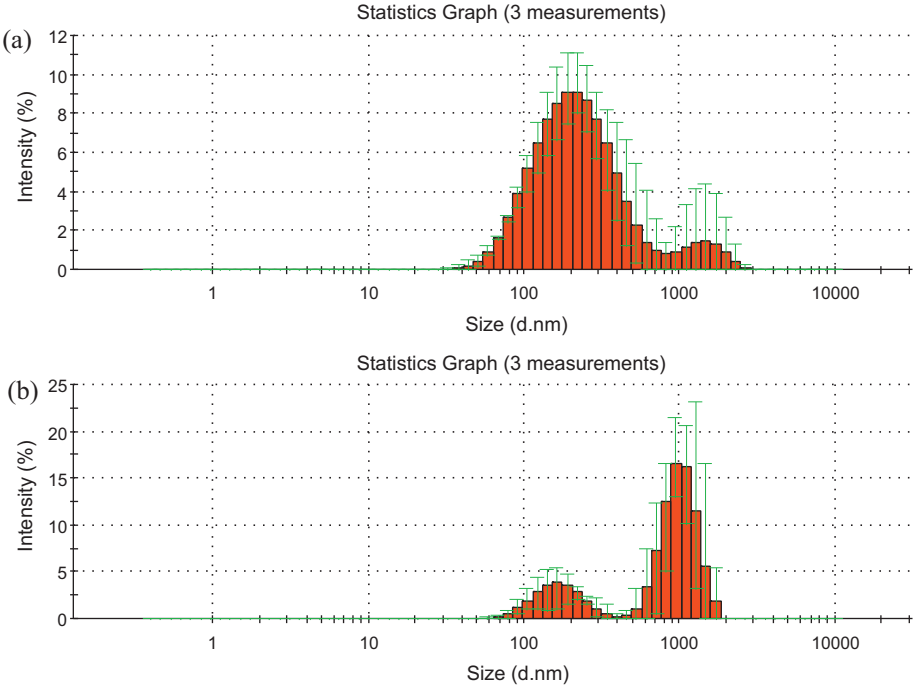

Fig. 5. Particle size distribution of CaP nanoshells using templates of (a) DOPA and (b) DPPA.

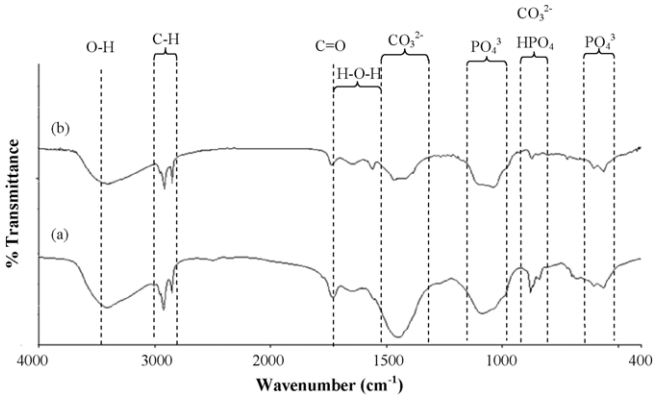

Fig. 6. FT-IR spectrum of CaP nanoshells using templates of (a) DOPA and (b) DPPA.

Fig. 6(a) and (b) shows the FTIR spectra of CaP nanoshells using DOPA and DPPA templates, respectively. The FTIR spectra of both CaP nanoshells had similar profiles. The peaks at 1043 cm^{-1} and 1088 cm^{-1} belong to the phosphate group (PO_4^{3-}) stretching mode [34] for CaPs nanoshells with DPPA and DOPA templates, respectively. Moreover, the peaks of the PO_4^{3-} bending mode splitting around 564 cm^{-1} and 605 cm^{-1} for both samples, indicating that CaP nanoshells with DOPA and DPPA templates were partially crystalline [34,43,44]. These results are in agreement with the EDX results, in which CaP nanoshells were partially crystalline or amorphous in structure. The peaks around 841 cm^{-1} for both samples were attributed to another phosphate group (HPO_4^{2-}) [44]. In addition, the stronger peaks of PO_4^{3-} in the CaP nanoshells with the DOPA template implied that it contains more phosphate ions compared to the CaP nanoshells with the DPPA template. These stronger peaks can contribute to the lower Ca/P molar ratio of CaP nanoshells using the DOPA template rather than the DPPA template. Moreover, the lower final molar ratio of Ca/P in the CaP nanoshells with the DOPA template may contain more phosphate [45]. Thus, the molar ratios obtained by EDX (Table 2) are in agreement with the results obtained by FT-IR in Fig. 6(a) and (b). Moreover, the presence of peaks in the region of 1400–1600 cm^{-1} and 869–879 cm^{-1} in the FT-IR spectra are attributed to carbonate groups (CO_3^{2-}) [43,46] due to the substitution of PO_4^{3-} by CO_3^{2} ions [47]. In addition, the carbonyl group (C=O) stretching vibration peak appeared at 1729 cm^{-1} and 1738 cm^{-1} for CaP nanoshells with DOPA and DPPA templates, respectively [48,49]. The C–H bonding of samples with liposome templates also appeared in the ranges of 2854–2925 cm^{-1} and 2850–2917 cm^{-1} for DOPA and DPPA templates, respectively [36,49]. The C=O and C–H bonding can be attributed to the carbon atom chain of the fatty acids of liposomes in CaP nanoshells. Moreover, strong peaks of the hydroxyl group (O–H) stretching were at 3394 cm^{-1} and 3411 cm^{-1} for CaP nanoshells with the DPPA template (Fig. 6(b)) and DOPA template (Fig. 6(a)), respectively [47]. The O–H in the samples also contributed to the polar headgroup (O–H) of the negative charge of liposomes. The peaks of CaP nanoshells with DOPA and DPPA templates around 1600 cm^{-1} [21] were described to H–O–H modes, indicating that water was absorbed on the surface [50]. As a result, all the peaks discussed above and their positions in the FTIR spectra confirm the formation of CaP nanoshells with both liposome templates (DOPA and DPPA).

3.3. Growth mechanism

Previous results show that liposomes play an important role in the formation of CaP nanoshells. Growth of CaPs with the presence of liposome templates is a heterogeneous nucleation process. Calcium ions are bound to the negatively charged of the phosphate headgroup (−OH) of liposomes. This negative charged headgroup in DOPA and DPPA templates can aid the localisation of ions surrounding the liposome [34].

Fig. 7(a) and (b) shows the growth mechanism of CaP nanoshells using DOPA and DPPA templates, respectively. In Fig. 7(a), there was an electrostatic attraction of calcium ions to the surface when CaPs were introduced to the DOPA template, resulting in a tightly bound stern layer of calcium ions on the surface of the DOPA template [36]. Thus, calcium and phosphate ions preferentially formed around the DOPA template when the areas around the DOPA template were saturated. Once CaPs surrounds the DOPA template, the shell may act as a normal nucleation site for further shell growth.

The results from the zeta potential analysis showed that the CaP nanoshells may become unstable after the growth of CaPs on the DPPA template. If the liposome is unstable, it is likely to deform or rupture as it complexes with precipitating ions [20]. Thus, the damaged structure of the DPPA template may occur during the experiments, especially during the drying process. Besides, the reaction between calcium and phosphate ions is also preferred over precipitation on the damaged DPPA template as the nucleation site. As a result, unlike CaP nanoshells using the DOPA template, the needle or irregular particles of CaPs were produced when using the DPPA template, as shown in TEM images (Fig. 4(b)).

The calcium ion is a bivalent cation and has strong electrostatic interaction with adjacent functional groups in solutions except for the interaction with the headgroup of the liposomes [51]. During drying, water evaporation could increase the concentrations of local free ions [20]. These free ions produce the van der Waals attractive forces that can overcome the electrostatic attraction of calcium ions with liposomes and influence the stability of liposomes (see Fig. 7(b)) because liposome stability is sensitive to the ionic strength of the surrounding milieu [22,52]. It might result in the two-dimensional growth of CaPs on the DPPA template rather than growth in all directions. In addition, the attractive van der Waals forces only caused the tendency towards aggregation in CaP nanoshells using the DOPA template. Fig. 8(a) and (b) shows the chemical structures of DOPA and DPPA templates, respectively. Both liposome templates may differ in the fatty acid part. The carbon atom chains of the DPPA template only contain single chemical bonds, while the DOPA template has double bonds in the carbon atom chains, which might be due to the higher stability of the DOPA template than DPPA template in the synthesis of CaP nanoshells.

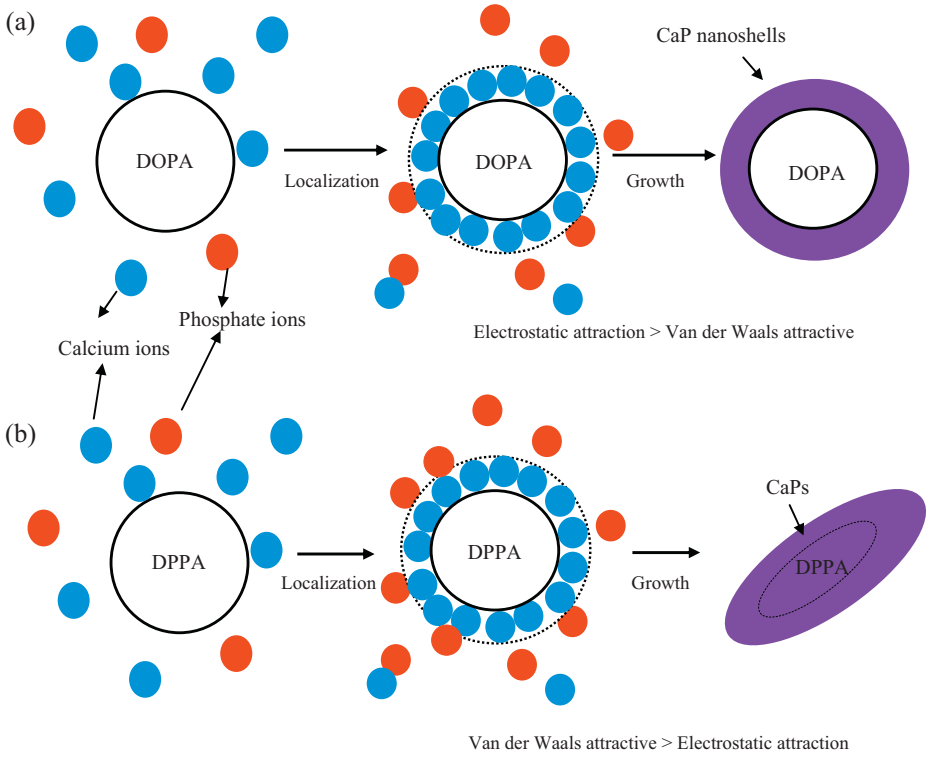

Fig. 7. Schematics for the growth mechanism of CaP nanoshells using liposome templates of (a) DOPA and (b) DPPA.

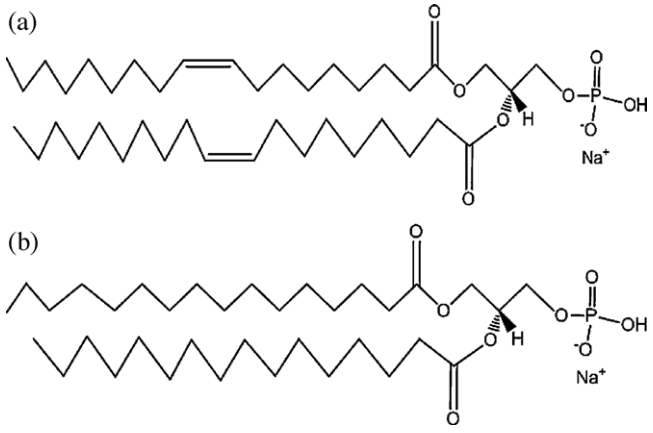

Fig. 8. Chemical structures of liposome templates of (a) DOPA and (b) DPPA.

4. Conclusion

CaP nanoshells were synthesised by using different liposomes as templates. The results showed that both DOPA and DPPA formed spherical nanoshell structures.

Based on the results obtained in the present investigation, the morphology and size of the CaP nanoshells depended on the types of template used. The results of morphological analysis showed that CaP nanoshells with spherical structures can be successfully formed by using the DOPA template. In contrast, the needle or irregularly shaped particles were observed in the CaP nanoshells using the DPPA template. The molar ratio of Ca/P of CaP nanoshells with the DOPA template (0.97) approached the expected molar ratio of the Ca/P of CaP nanoshells (1.00). This Ca/P molar ratio (1.00) could correspond to either crystalline brushite or ACP. On the other hand, CaP nanoshells using the DPPA template had a higher final molar ratio of Ca/P of (1.45), which corresponded to CDHA or ACP. However, CaP nanoshells using DOPA and DPPA templates were indicated as partially crystalline in FT-IR analyses. Thus, CaP nanoshells were demonstrated to be partially crystalline or amorphous in structure.

On the other hand, the results for the particle size distribution analysis showed that the CaP nanoshells produced using the DOPA template were more monodisperse than those using the DPPA template. In addition, the magnitude of the zeta potential of the surface of the average zeta potentials of CaP nanoshells decreased after the growth of CaPs on DOPA and DPPA templates. The result of the zeta potential of CaP nanoshells with the DPPA template (less negative than −30 mV) showed that the nanoshells may become unstable after the growth of CaPs on the DPPA template. This result was proven in the morphological analysis. It shows the effectiveness of liposomes depends on the stability. Conversely, CaP nanoshells using the DOPA template with zeta potential more negative than −30 mV were still considered stable. Thus, the stability of the liposome template is important in the synthesis of CaP nanoshells. Further study needs to be conducted to stabilise the liposome structure during the growth of CaP nanoshells.

Acknowledgements

The financial support provided by the British Council (UK Prime Minister's Initiative for International Education (PMI2)

Connect scheme), Universiti Sains Malaysia (Research University (RU) grant and Research University Postgraduate Research Grant Scheme (USM-RU-PRGS)) are gratefully acknowledged. Chiew Hwee Yeo also acknowledges a USM Fellowship for the support of her studies. The authors acknowledge helpful discussions with Prof. A.R. Boccaccini (University of Erlangen-Nuremberg, Germany).

References

[1] S.J. Kalita, A. Bhardwaj, H.A. Bhatt, Nanocrystalline calcium phosphate ceramics in biomedical engineering, Materials Science and Engineering C 27 (2007) 441–449.
[2] R.A. Mickiewicz, Polymer–Calcium Phosphate Composites for Use as an Injectable Bone Substitute, Department of Materials Science and Engineering, vol. Degree of Master of Science in Materials Science and Engineering, Massachusetts Institute of Technology, 2001.
[3] Y. Cai, R. Tang, Calcium phosphate nanoparticles in biomineralization and biomaterials, Journal of Materials Chemistry 18 (2008) 3775–3787.
[4] T.J. Webster, Nanophase ceramics: the future orthopedic and dental implant material, in: J.Y. Ying (Ed.), Nanostructured Materials, vol. 27, Academic Press, 2001.
[5] M.J. Mayo, R.W. Siegel, Y.X. Liao, W.D. Nix, Nanoindentation of nanocrystalline ZnO, Journal of Materials Research 7 (1992) 973–979.
[6] M.J. Mayo, R.W. Siegel, A. Narayanasamy, W.D. Nix, Mechanical properties of nanophase TiO_2 as determined by nanoindentation, Journal of Materials Research 5 (1990) 1073–1082.
[7] J.L. Xu, K.A. Khor, Y.W. Gu, R. Kumar, P. Cheang, Radio frequency (rf) plasma spheroidized HA powders: powder characterization and spark plasma sintering behavior, Biomaterials 26 (2005) 2197–2207.
[8] J.L. Xu, K.A. Khor, Z.L. Dong, Y.W. Gu, R. Kumar, P. Cheang, Preparation and characterization of nano-sized hydroxyapatite powders produced in a radio frequency (rf) thermal plasma, Materials Science and Engineering A 374 (2004) 101–108.
[9] S. Jinawath, P. Sujaridworakun, Fabrication of porous calcium phosphates, Materials Science and Engineering C 22 (2002) 41–46.
[10] W. Tjandra, P. Ravi, J. Yao, K.C. Tam, Synthesis of hollow spherical calcium phosphate nanoparticles using polymeric nanotemplates, Nanotechnology 17 (2006) 5988–5994.
[11] K. Wei, C. Lai, Y. Wang, Solvothermal synthesis of calcium phosphate nanowires under different pH conditions, Journal of Macromolecular Science. Part A: Pure and Applied Chemistry 43 (2006) 1531–1540.
[12] X. Du, Y. Chu, S. Xing, L. Dong, Hydrothermal synthesis of calcium hydroxyapatite nanorods in the presence of PVP, Journal of Materials Science 44 (2009) 6273–6279.
[13] J. Klesing, S. Chernousova, A. Kovtun, S. Neumann, L. Ruiz, J.M. Gonzalez-Calbet, M. Vallet-Regi, R. Heumann, M. Epple, An injectable paste of calcium phosphate nanorods, functionalized with nucleic acids, for cell transfection and gene silencing, Journal of Materials Chemistry 20 (2010) 6144–6148.
[14] M. Rezvannia, F. Moztarzadeh, M. Tahriri, Formation of hydroxyapatite nanoneedles on the surface of a novel calcium phosphate/blood plasma proteins biocement in simulated body fluid (SBF), Journal of Ceramic Processing Research 10 (2009) 669–673.
[15] N. Sounderya, Y. Zhang, Use of core/shell structured nanoparticles for biomedical applications, Recent Patents on Biomedical Engineering 1 (2008) 34–42.
[16] K. Kandori, N. Yamamoto, A. Yasukawa, T. Ishikawa, Preparation and characterization of disk-shaped hematite particles by a forced hydrolysis reaction in the presence of polyvinyl alcohol, Physical Chemistry Chemical Physics 4 (2002) 6116–6122.
[17] M. Epple, A. Kovtun, Functionalized calcium phosphate nanoparticles for biomedical application, Key Engineering Materials 441 (2010) 299–305.
[18] W. Chen, Z. Huang, Y. Liu, Q. He, Preparation and characterization of a novel solid base catalyst hydroxyapatite loaded with strontium, Catalysis Communications 9 (2008) 516–521.
[19] P. Wang, S.-W. Yook, S.-H. Jun, Y.-L. Li, M. Kim, H.-E. Kim, Y.-H. Koh, Synthesis of nanoporous calcium phosphate spheres using poly(acrylic acid) as a structuring unit, Materials Letters 63 (2009) 1207–1209.
[20] H.T. Schmidt, B.L. Gray, P.A. Wingert, A.E. Ostafin, Assembly of aqueous-cored calcium phosphate nanoparticles for drug delivery, Chem. Mater. 16 (2004) 4942–4947.
[21] M.Q. Chu, G.J. Liu, Preparation and characterization of hydroxyapatite/liposome core–shell nanocomposites, Nanotechnology 16 (2005) 1208–1212.
[22] H.T. Schmidt, A.E. Ostafin, Liposome directed growth of calcium phosphate nanoshells, Advanced Materials 14 (2002) 532–534.
[23] H.T. Schmidt, Calcium Phosphate Based Nanoshells for Use in Biomedical Applications, University of Notre Dame, Indiana, 2006, pp. 1–160.
[24] M.R. Mozafari, Liposomes: an overview of manufacturing techniques, Cellular & Molecular Biology Letters 10 (2005) 711–719.
[25] M.R. Mozafari, C.J. Reed, C. Rostron, C.P.E. Kocum, Construction of stable anionic liposome–plasmid particles using the heating method: a preliminary investigation, Cellular & Molecular Biology Letters 7 (2002) 923–927.
[26] S. Vemuri, C.T. Rhodes, Preparation and characterization of liposomes as therapeutic delivery systems: a review, Pharmaceutica Acta Helvetiae 70 (1995) 95–111.
[27] M.R. Mozafari, Nanoliposomes: preparation and analysis, in: V. Weissig (Ed.), Liposomes, Methods in Molecular Biology, vol. 605, Humana Press, a part of Springer Science + Business Media, 2010 , pp. 29–50.
[28] S.M. Schmidt, K.A. Moran, A.M.T. Kent, J.L. Slosar, M.J. Webber, M.J. McCready, C. Deering, J.M. Veranth, A. Ostafin, Uptake of calcium phosphate nanoshells by osteoblasts and their effect on growth and differentiation, Journal of Biomedical Materials Research Part A 87A (2008) 418–428.
[29] M. Sandstrom, Physico-Chemical Investigations of Bilayer Discs and Related Lipid Structures Formed in Liposomal Systems Intended for Triggered Release, Faculty of Science and Technology, Doctor of Philosophy, Uppsala University, Sweden, 2007, pp. 1–67.
[30] M.R. Mozafari, C. Johnson, S. Hatziantoniou, C. Demetzos, Nanoliposomes and their applications in food nanotechnology, Journal of Liposome Research 18 (2008) 309–327.
[31] M.M. Lapinski, A. Castro-Forero, A.J. Greiner, R.Y. Ofoli, G.J. Blanchard, Comparison of liposomes formed by sonication and extrusion: rotational and translational diffusion of an embedded chromophore, Langmuir 23 (2007) 11677–11683.
[32] M.O'. Doherty, Nanobiotechnology and Bioanalysis Group, What is liposome, vol. 2008, 2004.
[33] Malvern Instruments, Zeta potential: An Introduction in 30 minutes, Zetasizer Nano Series Technical Note (2010).
[34] Q. Xu, Y. Tanaka, J.T. Czernuszka, Encapsulation and release of a hydrophobic drug from hydroxyapatite coated liposomes, Biomaterials 28 (2007) 2687–2694.
[35] A.W. Pederson, J.W. Ruberti, P.B. Messersmith, Thermal assembly of a biomimetic mineral/collagen composite, Biomaterials 24 (2003) 4881–4890.
[36] H.T. Schmidt, M. Kroczynski, J. Maddox, Y. Chen, R. Josephs, A.E. Ostafin, Antibody-conjugated soybean oil-filled calcium phosphate nanoshells for targetted delivery of hydrophobic molecules, Journal of Microencapsulation 23 (2006) 769–781.
[37] M. Markovic, B.O. Fowler, W.E. Brown, Octacalcium phosphate carboxylates. 2. Characterization and structural considerations, Chemistry of Materials 5 (1993) 1406–1416.
[38] A. Rodrigues, A. Lebugle, Behavior in wet atmosphere of an amorphous calcium phosphate with an atomic Ca/P ratio of 1.33, Journal of Solid State Chemistry 148 (1999) 308–315.
[39] S.V. Dorozhkin, Calcium orthophosphates in nature, biology and medicine, Materials 2 (2009) 399–498.
[40] Malvern Instruments, Dynamic Light Scaterring: An Introduction in 30 minutes, DLS Technical Note (2010).
[41] S. McLaughlin, The electrostatic properties of membranes, Annual Review of Biophysics and Biophysical Chemistry 18 (1989) 113–136.

[42] J.T. Hautala, M.-L. Riekkola, S.K. Wiedmer, Anionic phospholipid coatings in capillary electrochromatography: binding of Ca^{2+} to phospholipid phosphate group, Journal of Chromatography A 1150 (2007) 339–347.
[43] A. Sugawara, S. Yamane, K. Akiyoshi, Nanogel-templated mineralization: polymer–calcium phosphate hybrid nanomaterials, Macromolecular Rapid Communications 27 (2006) 441–446.
[44] T. Hirai, M. Hodono, I. Komasawa, The preparation of spherical calcium phosphate fine particles using an emulsion liquid membrane system, Langmuir 16 (2000) 955–960.
[45] L. Sun, L.C. Chow, S.A. Frukhtbeyn, Preparation and properties of nanoparticles of calcium phosphates with various Ca/P ratios, Journal of Research of the National Institute of Standards and Technology 115 (2010) 245–255.
[46] Z.Z. Zyman, M.V. Tkachenko, D.V. Polevodin, Preparation and characterization of biphasic calcium phosphate ceramics of desired composition, Journal of Materials Science: Materials in Medicine 19 (2008) 2819–2825.
[47] P.N. Kumta, C. Sfeir, D.H. Lee, D. Olton, D. Choi, Nanostructured calcium phosphates for biomedical applications: novel synthesis and characterization, Acta Biomaterialia 1 (2005) 65–83.
[48] W. Zhang, Z.L. Huang, S.S. Liao, F.Z. Cui, Nucleation sites of calcium phosphate crystals during collagen mineralization, Journal of the American Ceramic Society 86 (2003) 1052–1054.
[49] R. Dluhy, D.G. Cameron, H.H. Mantsch, R. Mendelsohn, Fourier transform infrared spectroscopic studies of the effect of calcium ions on phosphatidylserine, Biochemistry 22 (1983) 6318–6325.
[50] M. Neupane, S. Lee, I. Park, H. Park, M. Lee, T. Bae, M. Yu, K. Lee, H. Kim, Influence of the number of carboxyl groups on the nucleation of hydroxyapatite, Metals and Materials International 16 (2010) 333–338.
[51] S. Singh, P. Bhardwaj, V. Singh, S. Aggarwal, U.K. Mandal, Synthesis of nanocrystalline calcium phosphate in microemulsion – effect of nature of surfactants, Journal of Colloid and Interface Science 319 (2008) 322–329.
[52] M. Zhang, K. Kataoka, Nano-structured composites based on calcium phosphate for cellular delivery of therapeutic and diagnostic agents, Nano Today 4 (2009) 508–517.